SF2A 2025
A. Siebert, K. Baillié, M. Béthermin, F. Cantalloube, E. Josselin, N. Lagarde, J. Malzac, J. Richard, L. Selliez, O. Venot (eds)

SEISMIC STUDY OF THE δ SCUTI STAR 38 ERI

L. Truffert-Tkalac[1], D. R. Reese[2] and L. Manchon[2]

Abstract. 38 Eri is a δ Scuti star with a projected equatorial velocity of nearly 100 km.s^{-1}. Its oscillations have been observed by various ground-based instruments as well as the MOST satellite, thus yielding their amplitudes and phases in different photometric bands. We compare the resultant amplitude ratios with theoretical predictions based on 2D rotating models and 2D oscillation calculations in an attempt to identify the modes. This enables us to constrain the fundamental parameters of the star, namely mass, radius, inclination, and rotation rate.

Keywords: asteroseismology, stars: oscillations, stars: rotation, stars: fundamental parameters, stars: individual: 38 Eri

1 Introduction

Interpreting the oscillation spectra of rapidly rotating stars has proven to be challenging because it is difficult to identify which theoretically calculated pulsation modes correspond to the observed ones. One way of overcoming this challenge is to measure the oscillations in different photometric bands and compare the resultant amplitude ratios and/or phase differences with theoretical predictions, since such signatures depend on the underlying mode geometry. The rapidly rotating δ Scuti star 38 Eri is an ideal target to which one can apply this technique as it has been observed by ground-based telescopes in the Strömgren *u, v, b, y* and Johnson-Cousins *U, B, V, R, I* bands, as well as by the MOST satellite thus leading to the detection of 18 modes (Paparó et al. 2018).

2 Modelling 38 Eri

In order to model 38 Eri, we used the classic constraints contained in Table 1 and some of the seismic constraints (10 frequencies and amplitude ratios in the Strömgren bands) from Paparó et al. (2018). As a first step, we fitted the amplitude ratios of individual modes using a grid of Self-Consistent Field (SCF) stellar models with rotation rates ranging from 0 to 0.5 $\Omega_{\rm C}$ in steps of 0.1 $\Omega_{\rm C}$, where $\Omega_{\rm C}$ is the critical break-up rotation rate (MacGregor et al. 2007). This involved interpolating mode visibilities to intermediate rotation rates, normalising them over the Strömgren bands, and comparing them with normalised observed amplitudes. Although, excellent fits of the individual amplitude ratios were obtained, this approach lead to multiple values of the rotation rate and inclination (see Fig. 1), rather than a single value as would be expected in a star.

Hence, as a second step, we applied the modelling strategy from Zwintz et al. (2019) which consists in fitting the frequencies and amplitude ratios of all of the modes simultaneously as well as the classic constraints using an MCMC approach (Foreman-Mackey et al. 2013) while interpolating in the grid of SCF models. We introduced an arbitrary error bar of 5 km.s^{-1} for the $v \sin i$ value (see Table 1), 0.01 mmag on the amplitudes and 0.001 c/d on the frequencies. We treated the rotation rate, inclination, mass, and radius as free parameters. From the mass and radius, we deduced an appropriate scale factor for the frequencies using a homologous transformation. Solutions for which the reduced $\chi^2_{\rm classic}$ exceeded three were rejected.

The left panel of Fig. 2 shows a corner plot with the MCMC samples obtained using classic constraints alone (grey scales) and using both classic and seismic constraints (blue). The best solution from this MCMC run is shown in right panel. As can be seen, it is difficult to fit the amplitude ratios (upper right panel) and frequency spectrum (lower right panel) simultaneously, while imposing a single inclination and rotation rate for the star.

[1] Université Paris Cité
[2] LIRA, Observatoire de Paris, Université PSL, Sorbonne Université, Université Paris Cité, CY Cergy Paris Université, CNRS, 92190 Meudon, France

Table 1. Classic constraints on 38 Eri (from Balona 2000).

Quantity	Value
$\log T_{\rm eff}$	3.85 ± 0.01
$\log L/L_\odot$	1.50 ± 0.04
$\log g$	3.60 ± 0.06
$v \sin i$	$98 \pm 5^\dagger$ km.s^{-1}

† We added this arbitrary error bar.

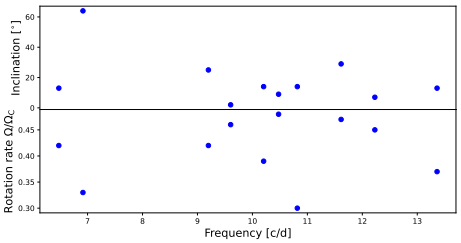

Fig. 1. Best stellar inclinations and rotation rates for modes fitted individually.

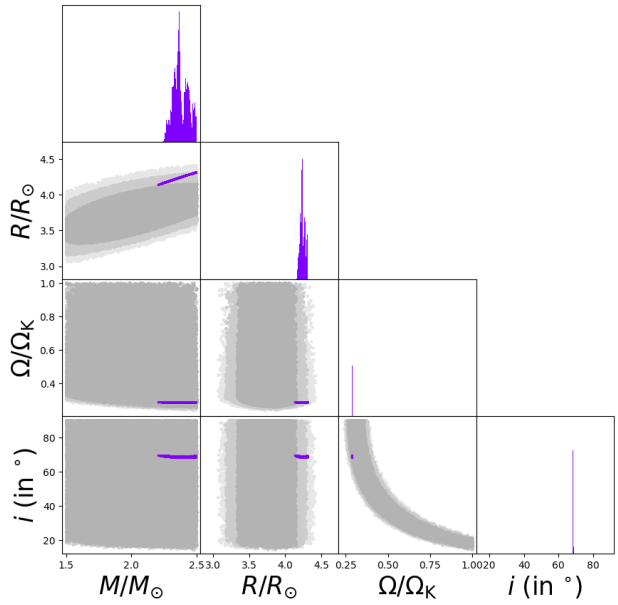

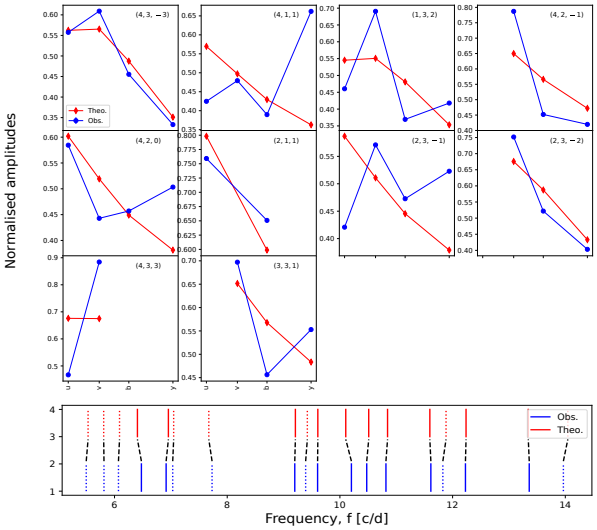

Fig. 2. Left: Triangle plot showing the solutions from an MCMC run. The grey-scale colours in the background correspond to MCMC solutions using the classic constraints alone whereas the blue regions correspond to solutions using classic and seismic constraints. **Right:** Observed (blue) and fitted (red) amplitude ratios and corresponding (n, ℓ, m) mode identifications from the best solution (upper plot). Observed and theoretical pulsation frequency spectra (lower plot). Continuous lines correspond to frequencies whose corresponding amplitude ratios have been fitted.

3 Conclusions

In order to improve the results, several possibilities exist. These include extending the grid of models to higher rotation rates, using ESTER models including the effects of stellar evolution (Mombarg et al. 2023), using the amplitudes in the Johnson-Cousins bands, and using non-adiabatic calculations to obtain more realistic mode visibilities.

We thank the organisers of the SF2A 2025!

References

Balona, L. A. 2000, MNRAS, 318, 289
Foreman-Mackey, D., Hogg, D. W., Lang, D., & Goodman, J. 2013, PASP, 125, 306
MacGregor, K. B., Jackson, S., Skumanich, A., & Metcalfe, T. S. 2007, ApJ, 663, 560
Mombarg, J. S. G., Rieutord, M., & Espinosa Lara, F. 2023, A&A, 677, L5
Paparó, M., Kolláth, Z., Shobbrook, R. R., et al. 2018, MNRAS, 477, 4362
Zwintz, K., Reese, D. R., Neiner, C., et al. 2019, A&A, 627, A28